

## Structure and Stability of Small Nitrile Sulfides and Their Attempted Generation from 1,2,5-Thiadiazoles

Tibor Pasinszki,<sup>\*,†</sup> Tamás Kárpáti,<sup>†</sup> and Nicholas P. C. Westwood<sup>\*,‡</sup>

Department of Inorganic Chemistry, Budapest University of Technology and Economics, H-1521 Budapest, Gellért tér 4, Hungary, and Guelph–Waterloo Centre for Graduate Work in Chemistry, Department of Chemistry and Biochemistry, University of Guelph, Guelph, Ontario, Canada N1G 2W1

Received: March 5, 2001; In Final Form: April 23, 2001

The gas-phase generation and spectroscopic identification of nitrile sulfides by thermolysis of 1,2,5-thiadiazole precursors was attempted, but in all cases the thiadiazoles were found to produce sulfur and the corresponding nitrile. This prompted an investigation by ab initio and density functional calculations for the equilibrium geometries, stabilities, and decomposition mechanisms of several nitrile sulfides (XCNS, where X = H, F, Cl, CN, CH<sub>3</sub>). Equilibrium geometries obtained from calculations at the B3LYP, MPn ( $n = 2-4$ ), QCISD, QCISD(T), CCSD, and CCSD(T) levels with moderate to large basis sets indicate that the molecules have linear heavy atom geometries. The exception is the fluoro derivative, which is bent with a calculated barrier to linearity of 889 cm<sup>-1</sup> (B3LYP/cc-pVTZ). The nitrile sulfides are predicted by the B3LYP method to be stable in the dilute gas phase, whereas in the condensed phase they are suggested to be very unstable due to bimolecular decomposition. The mechanism of this loss process is complicated by various sulfur transfer and cyclization reactions between decomposition intermediates, with the predicted stable products being sulfur, nitriles, and thiadiazoles. The first step of the bimolecular decomposition is either a cycloaddition to thiofuroxan or a sulfur transfer with simultaneous S<sub>2</sub> loss to nitriles.

### Introduction

Since the first indirect evidence for the existence of the first nitrile sulfide, XCNS (benzonitrile sulfide) in 1970,<sup>1</sup> these compounds have become important transient species and reactive intermediates in organic chemistry. Although much less stable than the corresponding nitrile oxides, to the extent that their isolation in the pure state is not possible, they have been used in 1,3-dipolar cycloaddition reactions in solution, providing routes to several classes of heterocycles accessible only with difficulty by other means.<sup>2</sup> They are usually generated in situ, in the presence of a dipolarophile, by thermal decomposition of a five-membered ring containing the CNS moiety. The method of choice generally involves thermolysis of substituted 1,3,4-oxathiazol-2-ones. The chemical trapping reactions provide the strongest evidence for the existence of nitrile sulfides, suggesting that the nitrile sulfide forms and then instantly reacts. Two reviews,<sup>2,3</sup> considering work up to about 1991, summarize their chemistry, mechanistic aspects, and some spectroscopy.

Spectroscopic studies on nitrile sulfides are limited due to their instability at room temperature. PhCNS and CH<sub>3</sub>CNS have been detected by infrared and ultraviolet spectroscopies when generated photolytically in a cold matrix or when the gas-phase pyrolysis products were condensed onto a cold window at cryogenic temperatures using matrix isolation techniques (see refs 2–4 and references therein). Nitrile sulfides are believed to be thermally unstable, readily losing sulfur; photolysis of nitrile sulfides at cryogenic temperatures or allowing the sample to warm above 100 K resulted in desulfuration.<sup>2</sup> The mechanism

of this process has been the subject of some debate and is not yet understood, although S<sub>2</sub> has been identified as being a primary product.<sup>2,3</sup>

The parent thiofulminic acid (HCNS) and other simple nitrile sulfide derivatives, e.g., PhCNS, NCCNS, CICNS, NH<sub>2</sub>CNS, and CH<sub>3</sub>CNS have recently been generated and identified as neutrals in the gas phase by neutralization–reionization mass spectroscopy (NRMS),<sup>3–7</sup> as have some of the corresponding seleno compounds (RCNSe).<sup>8,9</sup> In the case of the nitrile sulfides a beam of mass-selected nitrile sulfide ions, produced either by electron impact ionization and subsequent fragmentation of suitable five-membered heterocycles containing at least one CNS linkage, or by sulfur ion transfer from CS<sub>3</sub><sup>•+</sup> to the nitrogen atom of nitriles, is neutralized in a collision cell with Xe or NH<sub>3</sub> and then reionized in a second collision cell with O<sub>2</sub>. This method, which establishes the existence of the neutral species with lifetimes of at least microseconds in the dilute gas phase in the mass spectrometer, has no preparative value for nitrile sulfides. Because of the lack of successful methods to generate these molecules into the dilute gas phase in sufficient yield, no other spectroscopic data exist. The experimental structures of nitrile sulfides are thus unknown and methods to generate them into the gas phase would provide an important step toward their full electronic and geometric characterization.

Given the paucity of experimental investigations, quantum-chemical calculations can provide information on the structures and stabilities. Early ab initio Hartree–Fock (HF) calculations on HCNS predicted a linear structure,<sup>10</sup> which seemed to be in good agreement with the most frequently used mesomeric structure of nitrile sulfides (X–C≡N→S) which, with an sp carbon atom, suggests a linear formulation. This was challenged recently by MP2 calculations using various basis sets,<sup>7</sup> predicting a slightly bent equilibrium configuration. The structures of some

\* Authors for correspondence. E-mail: pasinszki.inc@chem.bme.hu; westwood@chembio.uoguelph.ca.

<sup>†</sup> Budapest University of Technology and Economics.

<sup>‡</sup> University of Guelph.

simple derivatives were also calculated at the MP2 level; the frame of NCCNS<sup>11</sup> and CH<sub>3</sub>CNS<sup>7</sup> was calculated to be linear, whereas the frame of CNCNS,<sup>11</sup> BrCNS,<sup>7</sup> ClCNS,<sup>6</sup> and NH<sub>2</sub>-CNS<sup>6</sup> was predicted to be bent. Barriers to linearity and potential quasi-linear behavior has not been investigated except for CNCNS;<sup>11</sup> this latter species being found to be quasi-linear with a calculated barrier to linearity of 139 cm<sup>-1</sup>. There is still no clear consensus on the structures of nitrile sulfides. They are anticipated to be linear or quasi-linear by analogy with nitrile oxides, but with calculated bond lengths sensitive to the bent-linear question; e.g., the calculated CN bond length varies between 1.140 and 1.208 Å in the various derivatives,<sup>6,7,10,11</sup> which cannot be explained by substituent effects. We note, and will show below, that neither MP2, which exaggerates the CN bond length and tends to bend the molecule, nor HF, which strongly underestimates the CN bond length, is the method of choice for calculating the structures of nitrile sulfides, and conclusions drawn on the basis of MP2 and HF calculations must be taken cum grano salis. Calculations on nitrile sulfides, as with the nitrile oxides,<sup>12,13</sup> are sensitive to electron correlation effects and the description of these latter effects is of crucial importance.

In this paper we report a quantum-chemical study on the equilibrium structures and stabilities of small nitrile sulfides (XCNS, where X = H (1), F (2), Cl (3), CN (4), CH<sub>3</sub> (5)), and their attempted generation from 1,2,5-thiadiazoles. These heterocycles were considered as potential precursors based on a recent report<sup>6</sup> of the formation of cyanogen *N*-sulfide (NCCNS) in the flash vacuum thermolysis (FVP, 750 °C) of 3,4-dicyano-1,2,5-thiadiazole. In addition, analogous heterocycles<sup>14</sup> were successfully used for the generation of unstable gas-phase nitrile oxides, particularly CH<sub>3</sub>CNO<sup>13</sup> and NCCNO<sup>15</sup> for which various spectroscopies (photoelectron and infrared in particular) provide unambiguous evidence for their detection and electronic and geometric structures. Of special computational interest are the structures and potential mechanisms for the decomposition of nitrile sulfides.

## Experimental Section

3,4-Dichloro-1,2,5-thiadiazole (6) was a commercial product (Aldrich). All other thiadiazole derivatives were synthesized according to known literature methods: 3,4-difluoro-1,2,5-thiadiazole (7) was synthesized from the dichloro-derivative with potassium fluoride,<sup>16</sup> 3,4-dicyano-1,2,5-thiadiazole (8) from diaminomaleonitrile with thionyl chloride,<sup>17</sup> 1,2,5-thiadiazole (9), and 3,4-dimethyl-1,2,5-thiadiazole (10) from ethylenediamine dihydrochloride and dimethylglyoxime, respectively, with sulfur monochloride.<sup>18</sup> 5-Methyl-1,3,4-oxathiazole-2-one (11) was synthesized from acetamide and ClC(O)SCL.<sup>19</sup>

For monitoring the gas-phase thermolysis and for identifying the pyrolysis products a combination of three different spectroscopic methods were used: He I photoelectron (PE), photoionization mass (PIMS), and infrared (IR) spectroscopies. He I (21.2 eV) PE spectra were obtained on a home-built fast pumping spectrometer<sup>20</sup> used to monitor in situ the products of fast flow thermolysis reactions. The capability exists for mass analyzing ions produced in the photoionization process using a quadrupole mass analyzer (Hiden Analytical, 320 amu) mounted directly above the photoionization point. The conventional EI source of the mass analyzer is removed, ionization being provided by He I or unfiltered HL (10.2–12.7 eV) radiation. Although not done in coincidence, PE and PIMS spectra can be recorded within seconds of each other; thus it is assumed that for a given PE spectrum the subsequent PIMS is of the same compound.

IR spectra were collected on a Nicolet 20SXC interferometer equipped with a 20 cm single pass cell. The cell, with KBr windows, gave a spectral range from 4000 to 400 cm<sup>-1</sup>. The effluent from the pyrolysis tube was pumped continuously through the cell using a rotary pump while maintaining the pressure constant between 400 and 500 mTorr.

## Computational Methods

The equilibrium structure of the parent nitrile sulfide, HCNS (1) was calculated at the HF, MP2, MP3, MP4, QCISD, QCISD(T), CCSD, and CCSD(T) levels using standard 6-31G\*\*, 6-311G(2d,2p), 6-311+G(3df,3pd), or cc-pVTZ basis sets, and also using density functional theory in the form of Becke's three-parameter exchange functional in combination with the Lee, Yang, and Parr correlation functional (B3LYP). The equilibrium geometries of the computationally larger derivatives, FCNS (2), ClCNS (3), NCCNS (4), and CH<sub>3</sub>CNS (5), were calculated at the B3LYP/cc-pVTZ level. Calculations for the stabilities (monomolecular and bimolecular sulfur loss) and decomposition mechanisms were performed at the B3LYP/6-31G\*\* level. The monomolecular sulfur loss was also calculated at the CCSD(T)(full)/cc-pVTZ//B3LYP/cc-pVTZ level. Equilibrium molecular geometries were fully optimized and harmonic vibrational frequencies were then calculated at the minimum energy geometries to confirm they were real minima on the potential energy surface (zero imaginary frequencies). Transitional states (TSs, first-order saddle points) were characterized with one imaginary frequency. All calculations were performed with the Gaussian-98 quantum chemistry package<sup>21</sup> implemented on Silicon Graphics Inc. Challenge/XL and Origin200 workstations.

## Results and Discussion

**Thermolysis of Thiadiazoles.** All of the following observations were confirmed by PE, PIMS, and IR measurements.

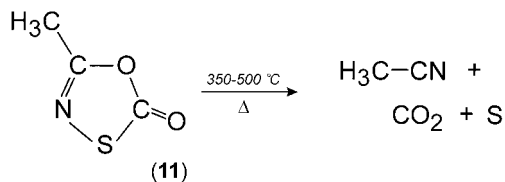
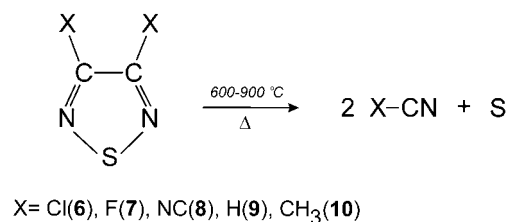
Thermolyses of thiadiazoles 6–10 were carried out in a quartz tube (8 mm i.d.) heated along 15 cm and attached directly to the spectrometer (PE/PIMS) or gas cell (IR); for a more efficient pyrolysis, the tube was loosely packed with quartz chips. We find that 1,2,5-thiadiazoles are thermally very stable, with the stability strongly influenced by the substituent. These thermolyses, however, did not produce identifiable nitrile sulfides, not even using 8, which was noted earlier<sup>6</sup> to produce 4 by FVP, one of the only nitrile sulfides, other than PhCNS,<sup>5</sup> to be generated by FVP, rather than in a mass spectrometer. The detection,<sup>6</sup> however, was by mass spectrometry, identification being based upon the observation of a decrease of the *m/z* intensity ratio of 136/84 by increasing the temperature of pyrolysis (0.8 at 200 °C and 0.6 at 750 °C). It is possible that this intensity change is due to secondary ion–molecule reactions and does not arise from the formation of 4. However, it is more likely that our present inability to observe 4 arises from a longer contact time in our furnace and, more particularly, from the higher pressures used in the present experiments, typically around 0.1–1 mTorr in the ionization region of the UPS experiment and ca. 450 mTorr in the FTIR cell. We note that the  $\nu_{\text{as/s}}(\text{CNS})$  IR bands of nitrile sulfides have a predicted large oscillator strength, expected to be distinctive for nitrile sulfides, much as the corresponding vibrations are important fingerprints for the nitrile oxide analogues.<sup>14</sup> However, we could not identify such bands in the IR spectra of the pyrolysates even after prolonged accumulation of the spectra.

The decomposition of thiadiazoles 6–10 rapidly and quantitatively produces nitriles and sulfur (Scheme 1) with the decomposition rate depending strongly on the substituent. The

**TABLE 1: Calculated Equilibrium Structure, Energies, Barrier to Linearity, Dipole Moment, and Rotational Constants of HCNS<sup>a</sup>**

	B3-LYP	MP2	MP3	MP4SDQ	MP4SDTQ	QCISD	QCISD(T)	CCSD	CCSD(T)
Barrier to Linearity									
basis set									
6-31G**	0	14	0	0	99	0	0	0	0
6-311G(2d,2p)	0	0	0	0	0	0	0	0	0
cc-pVTZ	0	0	0	0	11	0	<i>b</i>	<i>b</i>	<i>b</i>
6-311+G(3df,3pd)	0	0.3	0	0	14	0	0	0	0
Structure for the 6-311+G(3df,3pd) Basis Set									
H-C	1.062	1.062	1.061	1.063	1.066	1.063	1.065	1.063	1.064
C-N	1.159	1.180	1.150	1.158	1.185	1.157	1.167	1.155	1.167
N-S	1.596	1.574	1.600	1.607	1.584	1.609	1.601	1.609	1.601
HCN	180.0	174.1	180.0	180.0	165.0	180.0	180.0	180.0	180.0
CNS	180.0	179.0	180.0	180.0	177.3	180.0	180.0	180.0	180.0
tot. energy:	-491.65082	-491.13688	-491.13812	-491.14550	-491.18636	-491.14530	-491.17829	-491.14281	-491.17701
$\mu^c$	3.57	4.88	5.20	5.21	4.81	5.23	5.14	5.24	5.14
$B^d$	6.170	6.205	6.184	6.120	6.150	6.116	6.114	6.125	6.120

<sup>a</sup> Bond angles in degrees, bond lengths in angstroms, total energies in au, and barrier to linearity in cm<sup>-1</sup>; all of the electrons were included in the correlation energy calculations ("full"). <sup>b</sup> Not calculated. <sup>c</sup> Dipole moment in Debye. <sup>d</sup> Rotational constants in GHz; Isotopes: H-1, C-12, N-14, S-32.

**SCHEME 1**

dimethyl-substituted thiadiazole **10** is thermally the less stable. Decomposition of **10** commenced at 650 °C with increasing temperature, decreasing the amount of unreacted precursor, and at 900 °C the decomposition was complete. Other than the major products, acetonitrile and sulfur, a small amount of HCN was detected, its relative amount gradually increasing with temperature. Decomposition of **8** started above 700 °C, producing dicyanogen and sulfur. In each case, sulfur precipitated on the cold part of the glassware after the hot zone of the furnace. We found that unreacted precursor **8** could be trapped with a simple ice-water cooled U-trap inserted between the furnace and spectrometer. Thus, thermolysis of **8** could provide a simple and clean route to the on-line and small scale production of NCCN for spectroscopic investigations, thereby avoiding transport and storage of the highly poisonous NCCN gas. The decomposition of **9** commenced at 800 °C, but even at 900 °C the precursor composed the largest component, leaving the furnace. The formation of HCN and sulfur could be clearly observed. The halogen derivatives **6** and **7** were thermally even more stable; they did not decompose at 800 °C. Only a small amount of **6** decomposed at 900 °C, and the best indication of this was the precipitation of a small amount of sulfur on the glassware. We could not observe any sign of the thermal decomposition of **7** up to 900 °C.

Although mentioned earlier<sup>4</sup> that the FVP of 5-methyl-1,3,4-oxathiazole-2-one, **11**, does not produce acetonitrile sulfide, but acetonitrile, sulfur, and carbon dioxide, we repeated this work hoping that at a lower temperature we might identify formation

of the nitrile sulfide. Decomposition of **11** occurred at 350 °C and was complete at 500 °C, much lower temperatures than the substituted 1,2,5-thiadiazoles, **6**–**10**. No nitrile sulfide could be identified, **11** decomposing quantitatively to acetonitrile, sulfur, and carbon dioxide (Scheme 1), in agreement with the earlier investigation.

**Equilibrium Structure of Nitrile Sulfides.** Due to the lack of experimental data on the structures of nitrile sulfides, the reliability of the applied theoretical method cannot be tested by the usual procedure of comparing experiment and calculation. However, electron correlation and basis set effects are expected to be crucial much as they are in the case of the nitrile oxides<sup>12,13</sup> and so the smallest and computationally most tractable derivative, HCNS, **1**, was selected as a test case with its geometry calculated at various levels of theory and basis set size. Results are shown in Table 1.

**1** has a linear structure at all levels of theory and with all basis sets, except for MP2 and MP4 using 6-31G\*\*, cc-pVTZ, and 6-311+G(3df,3pd) basis sets. The barrier to linearity at MP2 and MP4 is, however, small and decreases with increasing basis set size. There is a linear–bent oscillation in the MP<sub>n</sub> expansion series; MP1 = HF(linear) → MP2(bent) → MP3(linear) → MP4(bent), which is also coupled to the bond lengths, especially the C≡N triple bond, for which oscillations can be seen in the MP<sub>n</sub> series. The C≡N bond lengths are 1.123, 1.180, 1.150, and 1.185 Å at the HF (not shown in Table 1), MP2, MP3, and MP4/6-311+G(3df,3pd) levels, respectively. The inclusion of triple effects in the calculations strongly lengthens CN; compare MP4SDQ vs MP4SDTQ, QCISD vs QCISD(T), and CCSD vs CCSD(T). Such observations are a strong indication of large and sensitive electron correlation effects and thus their description is of crucial importance. To provide an insight into the nature of the electron correlation problem, single point CISD(full) calculations were also done at the CCSD(T) geometry using the 6-311+G(3dp,3pd) basis set. The CISD wave function indicates that apart from the main HF configuration there is no other important configuration (weight of configurations larger than 0.05%: 93.6 (HF), 0.06, 0.06, 0.05, and 0.05%), and thus single reference post-HF methods should be sophisticated enough to describe the structure of **1**. The description of dynamic electron correlation, however, requires the use of high-level ab initio methods.

It is important to note that we have found previously similar strong electron correlation effects, demonstrated by an oscilla-

**TABLE 2: Calculated<sup>a</sup> Equilibrium Structure of Nitrile Sulfides, XCNS (X = H, F, Cl, NC, and CH<sub>3</sub>)**

	HCNS, <b>1</b>	FCNS, <sup>b</sup> <b>2</b>	CICNS, <b>3</b>	NCCNS, <b>4</b>	H <sub>3</sub> CCNS, <b>5</b>
X–C	1.061	1.296	1.625	1.349	1.449
C–N	1.160	1.186	1.163	1.171	1.159
N–S	1.603	1.589	1.609	1.577	1.619
N–C				1.161	
C–H					1.092
XCN	180.0	139.5	180.0	180.0	180.0
CNS	180.0	169.2	180.0	180.0	180.0
NCC				180.0	
HCC					110.5
tot. energy	–491.65340	–590.88996	–951.27123	–583.92544	–530.99779
$\mu^c$	3.57	1.32	3.89	1.42	5.28
$A^d$		206.578			159.982
$B$	6.135	2.562	1.522	1.498	2.406
$C$		2.530			2.406

<sup>a</sup> Calculated at the B3-LYP/cc-pVTZ level. Bond angles in degrees, bond lengths in angstroms, total energies in au. <sup>b</sup> Barrier to linearity is 888.6 cm<sup>-1</sup>. <sup>c</sup> Dipole moment in Debye. <sup>d</sup> Rotational constants in GHz. Isotopes: H-1, C-12, N-14, F-19, S-32, Cl-35.

**TABLE 3: Calculated<sup>a</sup> Vibrational Frequencies (cm<sup>-1</sup>) and Infrared Intensities (km/mol) of Nitrile Sulfides, XCNS (X = H, F, Cl, NC, and CH<sub>3</sub>)**

HCNS, <b>1</b> ( $C_{\infty v}$ )		FCNS, <b>2</b> ( $C_s$ )		CICNS, <b>3</b> ( $C_{\infty v}$ )		NCCNS, <b>4</b> ( $C_{\infty v}$ )		H <sub>3</sub> CCNS, <b>5</b> ( $C_{3v}$ )	
3478 (362.3)	$\nu_1$ (HC str)	2117 (64.0)	$\nu_1$ (CN str)	2286 (177.1)	$\nu_1$ (CN str)	2344 (575.0)	$\nu_1$ (str)	3084 (1.8)	$\nu_6$ (CH <sub>3</sub> as.str)
2142 (327.5)	$\nu_2$ (CN str)	1156 (480.4)	$\nu_2$ (CF str)	957 (163.6)	$\nu_2$ (NS str)	2201 (157.9)	$\nu_2$ (str)	3022 (18.0)	$\nu_1$ (CH <sub>3</sub> s str)
759 (50.7)	$\nu_3$ (NS str)	737 (86.0)	$\nu_3$ (NS str)	495 (2.8)	$\nu_3$ (CIC str)	1123 (93.4)	$\nu_3$ (str)	2316 (294.3)	$\nu_2$ (CN str)
429 (5.2)	$\nu_4$ (CNS def)	428 (108.4)	$\nu_4$ (CNS def)	370 (0.4)	$\nu_4$ (CNS def)	578 (22.8)	$\nu_4$ (str)	1468 (9.5)	$\nu_7$ (CH <sub>3</sub> as def)
365 (62.6)	$\nu_5$ (HCN def)	323 (0.4)	$\nu_6$ (CNS def)	79 (0.004)	$\nu_5$ (CICN def)	476 (0.5)	$\nu_5$ (def)	1414 (8.6)	$\nu_3$ (CH <sub>3</sub> s def)
		209 (54.6)	$\nu_5$ (FCN bend)			410 (7.4)	$\nu_6$ (def)	1043 (2.5)	$\nu_8$ (CH <sub>3</sub> rock)
						121 (4.9)	$\nu_7$ (CCN def)	1039 (64.4)	$\nu_4$ (str)
								591 (29.0)	$\nu_5$ (str)
								426 (0.5)	$\nu_9$ (CNS def)
								148 (1.3)	$\nu_{10}$ (CCN def)

<sup>a</sup> Calculated at the B3-LYP/cc-pVTZ level; unscaled frequencies.

**TABLE 4: Calculated Vertical Ionization Potentials (in eV) of Nitrile Sulfides, XCNS<sup>a</sup>**

HCNS, <b>1</b>	FCNS, <b>2</b>	CICNS, <b>3</b>	NCCNS, <b>4</b>	H <sub>3</sub> CNS, <b>5</b>	MO character
8.98 (8.89) $\pi$	9.27 (9.44) a'' 9.52 (9.46) a'	8.67 (8.75) $\pi$	9.66 (9.64) $\pi$	8.37 (8.38) e	$\pi_{nb}$ (CNS)
14.86 (16.51) $\pi$	13.92 (1617) a' 14.33 (16.56) a''	13.46 (14.85) $\pi$	13.20 (14.75) $\pi$	14.00 (15.44) e	$\pi_b$ (CNS)
			13.97 (17.17) $\sigma$ 15.74 (18.01) $\pi$		$n_N$ $\pi$ (NC)
15.72 (17.12) $\sigma$	16.30 (17.91) a'	15.57 (17.10) $\sigma$ 15.69 (17.74) $\pi$	16.65 (18.18) $\sigma$	15.12 (16.60) a <sub>1</sub>	$n_S$ (S lone pair)
				16.35 (18.01) e 17.35 (19.65) a <sub>1</sub>	$n_{Cl}$ CH <sub>3</sub> CH <sub>3</sub> C–Cl
		18.75 (21.01) $\sigma$			

<sup>a</sup> Calculated using the ROVGF/cc-pVTZ method at the B3LYP/cc-pVTZ geometries; Koopmans' IPs are in parentheses.

tory behavior in the MPn expansion series, basis set, barrier height, and total energy, on calculated properties of the nitrile oxide analogues.<sup>12,13,15,22,23</sup> The other effect, triple excitations markedly lengthening the C≡N bond length and tending to bend the structure, were also observed for nitrile oxides. It seems that the computational behavior of nitrile sulfides is very similar to that of nitrile oxides, which, given the structural similarity, is not surprising. The possibility of oscillatory behavior of the MPn series is known; starting from MP1 in the MPn series, MP2 exaggerates the effects of the new incoming terms, the double excitations, MP3 underestimates these due to DD coupling, MP4 exaggerates the new triple effects, and MP5 underestimates these due to TT coupling.<sup>24</sup> It seems that MP4SDTQ strongly overestimates the C≡N bond lengths and barrier height, in accord with the known fact that the method exaggerates triples contributions to the correlation energy.<sup>25</sup>

What has emerged from calculation of structural properties of nitrile oxides is the requirement for extra large basis sets and very high levels of theory, making nitrile oxides a serious

computational challenge. Calculations on **1** in this work suggest the same for nitrile sulfides. We note that if very high level conventional ab initio calculations are not feasible, DFT (e.g., in the form of B3LYP) can provide a reliable alternative. We have found DFT to give surprisingly good results for ground-state geometries and vibrational frequencies of nitrile oxides.<sup>12,15</sup> Calculations on **1** predict the same for nitrile sulfides; compare the B3LYP and CCSD(T) results in Table 1. For this reason we will use the B3LYP method for calculation of the geometries of substituted nitrile sulfides and for evaluating the decomposition process. To assist in detection of **1** by high-resolution techniques, Table 1 also includes the calculated dipole moments and rotational constants for all levels of theory.

Table 2 shows the calculated B3LYP/cc-pVTZ geometry, dipole moments, and rotational constants for molecules **1–5**, with the calculated IR frequencies and intensities and the ionization potentials (IPs) listed in Tables 3 and 4, respectively. The calculated unscaled vibrational frequency (2316 cm<sup>-1</sup>) for  $\nu$ (CN) in **5** is in very good agreement with that observed (2230



$\text{cm}^{-1}$ ) by matrix IR.<sup>3,4</sup> **1**, **3**, **4**, and **5** have a linear X—C—N—S frame, and only the fluoro derivative, **2**, is bent with a barrier to linearity of  $889\text{ cm}^{-1}$ . The similarity to the nitrile oxides must be noted again; FCNO is predicted to have a bent structure (barrier to linearity is  $1092\text{ cm}^{-1}$  at an identical level of theory),<sup>26</sup> but all other substituted nitrile oxides can be described with a linear or quasi-linear frame.<sup>14</sup> The propensity for bending in XCNO species increases with the increase in electronegativity of the substituent attached to the —CNO group and the increase in the C≡N bond length shows the same trend.<sup>14,26</sup> This can be seen in Table 2 for nitrile sulfides as well. From a comparison of the bond lengths of **1–5** with those of molecules having typical single and double N—S bonds ( $\text{H}_2\text{NSH}$  and  $\text{HNS}$ ) and double and triple CN bonds ( $\text{H}_2\text{CNH}$  and  $\text{HCN}$ ),<sup>27</sup> the CN bond in nitrile sulfides is found to lie close to a triple bond with the NS bond being close to a double bond. Calculated bond orders for CN and NS bonds are 2.6–2.9 and 1.7–2.0, respectively, using Gordy's rule.<sup>28</sup>

**Stability and Decomposition Mechanism of Nitrile Sulfides.** The thermal and photochemical instability of nitrile sulfides is well-known; photolysis at cryogenic temperatures or allowing the sample to warm above 100 K results in desulfuration.<sup>2,3</sup> The decomposition, however, seems not to be a simple unimolecular reaction. In solution, the decay rate is strongly concentration dependent, and the yields of 1,3-dipolar cycloaddition products are dilution dependent.<sup>29</sup> Isolated samples of nitrile sulfides are stable only in an inert solid matrix at low temperature. For example, upon heating, in EPA glass PhCNS is consumed as soon the glass melts (around 140 K), but in a rigid PVC matrix the decomposition is gradual and traces of the compound are detectable at room temperature for a short period of time.<sup>30,31</sup> Since the experimental observations are inconsistent with a unimolecular decomposition process, it has been suggested<sup>29</sup> that the decomposition is accelerated by reaction with short sulfur chains (e.g.,  $\text{S}_1\text{--}\text{S}_7$ ), i.e., by a sulfur transfer reaction, where the sulfur is expected to be extruded initially as an S atom. The formation of  $\text{S}_2$  is often observed in the pyrolysis mass spectrometry studies, and mechanisms involving dimerization or sulfur atom transfer have been postulated.<sup>3</sup>

Although clear from the accumulated experimental data<sup>3</sup> that the decomposition of nitrile sulfides follows higher order kinetics, the mechanism of this process is still not known. To clarify these questions, calculations have been performed using the B3LYP method. The first question considered was that of single sulfur atom formation, i.e., the direct rupture of the N—S bond:  $\text{XCNS} \rightarrow \text{XCN} + \text{S}$ . The formation of ground-state XCN and ground-state sulfur  $\text{S}(^3\text{P})$  in this process is spin-forbidden. According to our CCSD(T)(full)/cc-pVTZ//B3LYP/cc-pVTZ calculations, the spin-allowed extrusion of a singlet sulfur atom,  $\text{S}(^1\text{D})$ , is endothermic, requiring quite high energies of 58.3, 51.4, 55.8, 63.7, and 58.6 kcal/mol ( $\Delta E$ ) for **1–5**, respectively. Even formation of  $\text{S}(^3\text{P})$  would be endothermic with energies of 27.0, 20.2, 24.6, 32.5, and 27.5 kcal/mol for **1–5**, respectively. The calculations demonstrate that direct sulfur atom formation from nitrile sulfides cannot happen at low or ambient temperatures. As noted from experiment,<sup>3</sup> for example, the activation energy for unimolecular decomposition cannot be small; otherwise, it would not be possible to matrix isolate nitrile sulfides formed by FVP.

Potential bimolecular reactions were thus considered to account for the thermal instability of nitrile sulfides. B3LYP/6-31G\*\* calculations were performed first for **1**, the computationally most tractable species, with more than forty reactions

**TABLE 5: Energetics (in kcal/mol) of Reactions between HCNS and Decomposition Intermediates<sup>a</sup>**

No.	Reaction	$\Delta E$	$\Delta G$	$\Delta E^\ddagger$	$\Delta G^\ddagger$
1	$\text{HCNS} \rightarrow \text{HCN} + \text{S}$	+70.8	+73.0	70.8	73.0
2	$2\text{HCNS} \rightarrow 2\text{HCN} + \text{S}_2$	-8.7	-17.7	17.9	25.2
3	$2\text{HCNS} \rightarrow \begin{array}{c} \text{H} \\   \\ \text{S}=\text{N} \\   \\ \text{C}=\text{C} \\   \\ \text{H} \end{array}$	-11.3	-2.4	2.0	9.6
4	$\begin{array}{c} \text{H} \\   \\ \text{S}=\text{N} \\   \\ \text{C}=\text{C} \\   \\ \text{H} \end{array} \rightarrow \begin{array}{c} \text{S} \\   \\ \text{N} \\   \\ \text{S} \end{array}$	-30.6	-29.1	11.8	12.5
5	$\begin{array}{c} \text{S} \\   \\ \text{N} \\   \\ \text{S} \end{array} \rightarrow \begin{array}{c} \text{S} \\   \\ \text{N} \\   \\ \text{S} \end{array} + \text{S}$	+70.3	+72.2	70.3	72.2
6	$2\begin{array}{c} \text{S} \\   \\ \text{N} \\   \\ \text{S} \end{array} \rightarrow \begin{array}{c} \text{S} \\   \\ \text{N} \\   \\ \text{S} \end{array} + \begin{array}{c} \text{S} \\   \\ \text{S} \\   \\ \text{S} \end{array}$	-13.4	-13.8	3.1	13.2
7	$\begin{array}{c} \text{S} \\   \\ \text{N} \\   \\ \text{S} \end{array} \rightarrow \begin{array}{c} \text{S} \\   \\ \text{N} \\   \\ \text{S} \end{array} + \text{S}_2$	+3.7	-5.7	0.7	0.3
8	$\text{HCNS} + \begin{array}{c} \text{S} \\   \\ \text{N} \\   \\ \text{S} \end{array} \rightarrow \begin{array}{c} \text{S} \\   \\ \text{N} \\   \\ \text{S} \end{array} + \text{HCN}$	-13.6	-13.1	7.0	16.6
9	$\text{HCNS} + \text{S}_2 \rightarrow \begin{array}{c} \text{S} \\   \\ \text{S} \\   \\ \text{S} \end{array}$	-48.5	-39.2	-	-
10	$\text{HCNS} + \text{S}=\text{S}=\text{S} \rightarrow \begin{array}{c} \text{S} \\   \\ \text{S} \\   \\ \text{S} \end{array}$	-40.6	-29.0	-	-
11	$\text{HCNS} + \text{S}=\text{S}=\text{S} \rightarrow \begin{array}{c} \text{S} \\   \\ \text{S} \\   \\ \text{S} \end{array} + \text{HCN}$	-34.7	-33.7	11.8	19.6
12	$\text{HCNS} + \begin{array}{c} \text{S} \\   \\ \text{S} \\   \\ \text{S} \end{array} \rightarrow \begin{array}{c} \text{S} \\   \\ \text{N} \\   \\ \text{S} \end{array} + \text{HCN}$	-10.6	-10.0	9.4	17.4
13	$\begin{array}{c} \text{S} \\   \\ \text{N} \\   \\ \text{S} \end{array} + \begin{array}{c} \text{S} \\   \\ \text{S} \\   \\ \text{S} \end{array} \rightarrow \begin{array}{c} \text{S} \\   \\ \text{N} \\   \\ \text{S} \end{array} + \begin{array}{c} \text{S} \\   \\ \text{S} \\   \\ \text{S} \end{array}$	-11.1	-10.8	6.9	18.5
14	$\text{HCNS} + \begin{array}{c} \text{S} \\   \\ \text{S} \\   \\ \text{S} \end{array} \rightarrow \text{HCN} + \begin{array}{c} \text{S} \\   \\ \text{S} \\   \\ \text{S} \end{array}$	-34.3	-33.6	-	-
15	$\begin{array}{c} \text{S} \\   \\ \text{S} \\   \\ \text{S} \end{array} + \text{S}_2 \rightarrow \begin{array}{c} \text{S} \\   \\ \text{S} \\   \\ \text{S} \end{array}$	-13.7	-4.7	-	-
16	$\begin{array}{c} \text{S} \\   \\ \text{S} \\   \\ \text{S} \end{array} \rightarrow \begin{array}{c} \text{S} \\   \\ \text{S} \\   \\ \text{S} \end{array}$	-22.7	-21.5	5.4	6.4
17	$\text{HCNS} + \text{HCN} \rightarrow \begin{array}{c} \text{S} \\   \\ \text{N} \\   \\ \text{S} \end{array}$	-42.4	-32.3	16.5	25.0
18	$\text{S}=\text{S}=\text{S} + \text{HCN} \rightarrow \begin{array}{c} \text{S} \\   \\ \text{N} \\   \\ \text{S} \end{array}$	-5.4	+5.3	11.5	21.8
19	$\text{HCNS} + \begin{array}{c} \text{S} \\   \\ \text{N} \\   \\ \text{S} \end{array} \rightarrow \begin{array}{c} \text{S} \\   \\ \text{N} \\   \\ \text{S} \end{array} + \text{HCN}$	+27.6	+28.6	23.8	32.5
20	$\text{HCNS} + \begin{array}{c} \text{S} \\   \\ \text{N} \\   \\ \text{S} \end{array} \rightarrow \begin{array}{c} \text{S} \\   \\ \text{N} \\   \\ \text{S} \end{array} + \text{HCN}$	+0.5	+0.8	14.3	23.3

<sup>a</sup> Calculated at the B3LYP/6-31G\*\* level; relative energies ( $\Delta E$ ), relative Gibbs free energies ( $\Delta G$ ), and energy barriers ( $\Delta E^\ddagger$ ,  $\Delta G^\ddagger$ ), are relative to the sum of the energies (corrected with ZPE) or Gibbs free energies of starting materials. Gibbs free energies are calculated at 298.15 K and 1 atm. Hydrogen atoms are omitted on rings for simplicity.

between **1** and various reaction products considered including characterization of the minima and transition states along the reaction paths. The most important reactions and their energetics are listed in Table 5, and the essence of the decomposition process of **1** is summarized in Figure 1.

As the initiating step, two bimolecular decomposition reactions are found for **1**, one via S—S and the other via C—C. In the first, which is kinetically less favored, two molecules of **1** produce two molecules of nitrile (HCN) and singlet  $\text{S}_2$  directly

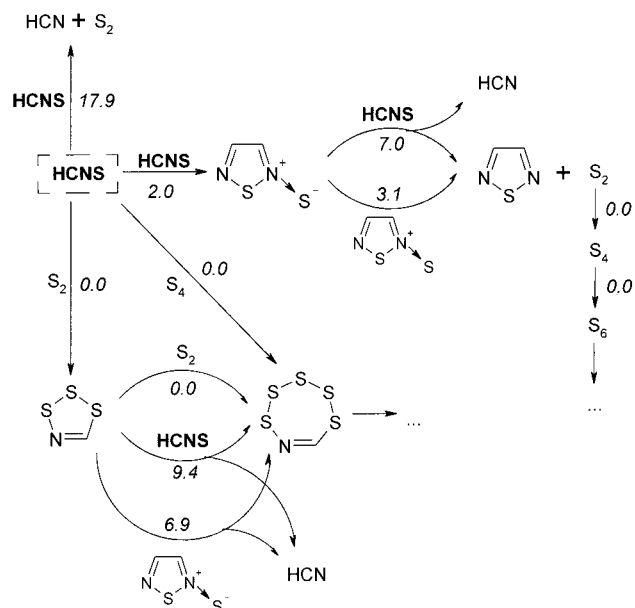


**Figure 1.** Decomposition of HCNS (**1**) (kinetic energy barriers for reactions,  $\Delta E^\ddagger$ , are shown in kcal/mol).

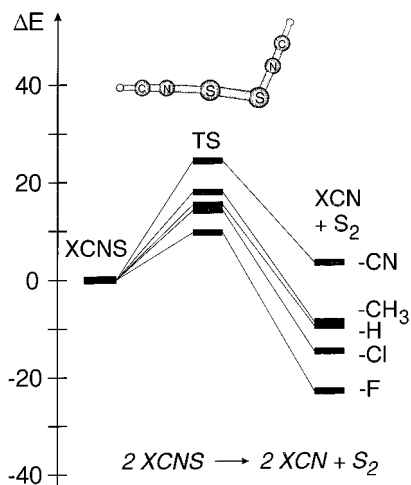


**Figure 2.** Bimolecular decomposition of nitrile sulfides, XCNS (X = H (**1**), F (**2**), Cl (**3**), CN (**4**), CH<sub>3</sub> (**5**)), in a “tail to tail” reaction. Energies ( $\Delta E$ , in kcal/mol) are relative to that of the sum of total energies of two XCNS molecules (ZPE included).

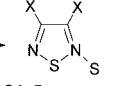
in a “tail to tail” (HCNS...SNCH) reaction after passing over a kinetic energy barrier of 17.9 kcal/mol ( $\Delta E^\ddagger$ ;  $\Delta G^\ddagger = 25.2$  kcal/mol at 273.15 K and 1 atm; reaction number R2, Table 5; see the TS structure in Figure 2). There is no intermediate in this reaction, and the two N–S bonds simultaneously break, releasing S<sub>2</sub> and the nitrile. Thus, this is not a simple sulfur atom transfer, as was suggested earlier,<sup>29</sup> and calculations show that a suggested intermediate such as HCNS<sub>2</sub> does not exist on the singlet potential energy surface. In the second route, two molecules of **1** dimerize into 2-sulfo-1,2,5-thiadiazole (thiofuroxan) in a typical Firestone-type [2+3] cycloaddition reaction (R3, R4). The kinetic energy barrier of the first step (TS1) leading to the Firestone intermediate (IM) is a mere 2.0 kcal/mol, which clearly explains the instability of **1** if molecules interact with each other, e.g., in the condensed phase, and may explain our inability to observe nitrile sulfides under our present experimental conditions. This dimerization is very similar to the known dimerization of nitrile oxides leading to stable furoxans,<sup>12,13,26</sup> with the major difference, as we show below, that thiofuroxan can readily react further and can also take part

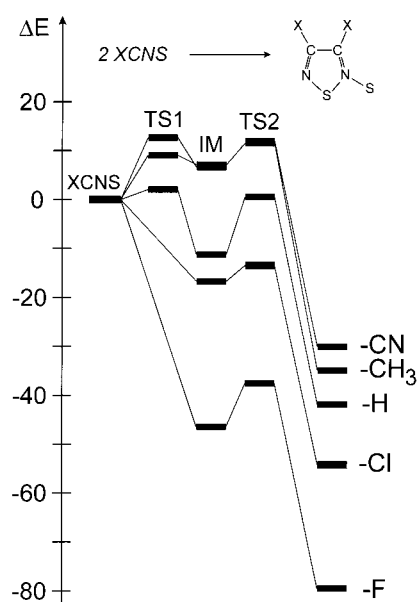
in the desulfuration process of **1**. Thiofuroxan, like **1**, does not lose sulfur in a monomolecular process (R5) and should be stable under isolated conditions, i.e., in the dilute gas phase or in an inert solid matrix. In this context, a NCCNS dimer was seen in the mass spectroscopy work.<sup>6</sup> Thiofuroxan loss can, however, occur in bimolecular processes by reaction with another molecule of thiofuroxan (R6, R7) producing singlet S<sub>2</sub> and thiadiazole or with **1** (R8, R7) producing singlet S<sub>2</sub>, thiadiazole, and HCN with barriers of 3.1 and 7.0 kcal/mol, respectively. These reactions involve the intermediacy of a kinetically very unstable sulfurated thiofuroxan (R7). S<sub>2</sub> is a key intermediate in the decomposition of **1**. Either it reacts with other short sulfur chains without any kinetic energy barrier to form S<sub>4</sub>, S<sub>6</sub>, S<sub>8</sub>, etc., or more importantly, it reacts with **1** without any barrier, forming a five-membered ring cycloadduct (R9). Other short sulfur chains, like S<sub>4</sub>, react with **1** similarly and form cycloadducts; in the case of S<sub>4</sub> a seven-membered ring containing five sulfur atoms forms (R10). Sulfur chains S<sub>n</sub>, longer than S<sub>2</sub>, can also react with **1** with the formation of HCN and S<sub>n+1</sub> (e.g. R11), but this is kinetically less favored than the cycloaddition (R10). The sulfur-containing rings formed, e.g., in reactions R9 and R10 are good sulfur scavengers, remove sulfur from **1** (R12) or from thiofuroxan (R13) in two steps, and grow into a larger sulfur-containing ring (see R12 → R14) or react with S<sub>2</sub> to form the same larger ring (see R15 → R16). We have also investigated whether the stable reaction products thiadiazole and HCN could react with any component of the complicated reaction mixture, particularly since **1** is a good 1,3-dipolarophile and HCN is a 1,2-dipolarophile. The reaction between **1** and HCN is exothermic but has a kinetic barrier of 16.5 kcal/mol (R17); therefore the reaction is not expected to proceed at low temperatures, but at room or higher temperatures this could contribute to an increase in the yield of thiadiazole product. The reaction of HCN with sulfur chains is endothermic, thus thermodynamically not favored (e.g., R18). The reaction between thiadiazole and **1**, a possible sulfur transfer, is also endothermic and not favored (R19, R20).

Summarizing the decomposition mechanism of **1**, calculations show that the initiating steps are, consecutively, the cycloaddition of **1** and the decomposition of thiofuroxan with the formation of S<sub>2</sub>. Short sulfur chains effectively remove sulfur from **1** and grow larger and larger in the cycloaddition and sulfur transfer processes discussed above and produce the corresponding nitrile (HCN). Large rings containing one HCN unit could possibly eliminate HCN at the end, but this could not be investigated due to computational limitations. It is interesting to note that the calculations suggest that besides sulfur and nitrile (HCN), thiadiazole also forms in the decomposition of nitrile sulfide. This latter product has never been considered in previous work.

The decomposition of **1** is a complicated process and follows higher order kinetics. It is an interesting question how substituents on the nitrile sulfide group influence this. Because of the large number of potential reaction routes, it was not possible to calculate decomposition mechanisms for **2**–**5** in detail, similar to those described for **1**, but the key first steps, cycloaddition or “tail to tail” reactions between nitrile sulfides, is discussed here. Results are shown in Figures 2 and 3 with calculated reaction heats and kinetic energy barriers listed in Table 6. As the results show, the cycloaddition (thiofuroxan route, Figure 3) for nitrile sulfides is both kinetically and thermodynamically much more favored than the direct singlet S<sub>2</sub> loss in the “tail to tail” reaction (Figure 2). There is no energy barrier for the cycloaddition of **2** and **3**, the barrier is a mere 2.0 kcal/mol for

**TABLE 6: Calculated Reaction Heat ( $\Delta E$ ,  $\Delta G$ ) and Reaction Barriers ( $\Delta E^\ddagger$ ,  $\Delta G^\ddagger$ ) for the Decomposition of Nitrile Sulfides (XCNS, X = H, F, Cl, CN, and CH<sub>3</sub>)<sup>a</sup>**

molecule	$\Delta E$	$\Delta G$	$\Delta E^\ddagger$	$\Delta G^\ddagger$
$2XCNS \rightarrow 2XCN + S_2$				
1	-8.7	-17.7	17.9	25.2
2	-22.9	-30.4	9.6	18.7
3	-14.7	-22.3	14.3	23.4
4	+3.4	-5.4	24.3	30.9
5	-9.5	-18.8	15.3	21.3
$2XCNS \rightarrow$ 				
1	-41.9	-31.5	2.0	9.6
2	-79.5	-66.5		
3	-54.2	-41.0		
4	-30.1	-19.1	12.6	21.1
5	-34.9	-23.0	9.0	18.4

<sup>a</sup> Calculated at the B3LYP/6-31G\*\* level; in kcal/mol.**Figure 3.** Cycloaddition of nitrile sulfides, XCNS (X = H (1), F (2), Cl (3), CN (4), CH<sub>3</sub> (5)). Energies ( $\Delta E$ , in kcal/mol) are relative to that of the sum of total energies of two XCNS molecules (ZPE included). In the case of the energetically close CN and CH<sub>3</sub> substituted molecules, the lower barrier for TS1 corresponds to -F.

1, and it is 12.6 and 9.0 kcal/mol for 4 and 5, respectively, which suggests possible dimerization at less than room temperature, especially for 1–3, and would explain the instability of nitrile sulfides. It is interesting to note that the kinetic barrier to dimerization decreases with an increasing electronegativity of the substituents, i.e., in the order CH<sub>3</sub> > H > Cl > F. The cyano-substituted derivative, 4, seems to be an exception in this series and is predicted to be the less unstable. The completely delocalized electronic structure of 4 might be an explanation for this, but this has not been investigated in this work. Such relative enhanced stability has been noted for NCCNO<sup>14,32</sup> when compared to the other nitrile oxides. Calculations suggest that attaching a strong electron donating, sterically large, possibly aromatic substituent to the nitrile sulfide group increase the kinetic stability.

## Conclusion

This work has sought to generate nitrile sulfides, XCNS (where X = H, F, Cl, CN, CH<sub>3</sub>), in the gas phase for

spectroscopic investigations by thermolyzing 1,2,5-thiadiazoles, but in all cases the thiadiazoles were found to produce sulfur and the corresponding nitrile. This prompted a theoretical investigation for the structures, stabilities, and decomposition mechanisms of nitrile sulfides. Calculations indicate that the molecules have linear heavy atom geometries, the exception is the fluoro derivative, which is bent with a calculated barrier to linearity of 889 cm<sup>-1</sup>. Calculations on the nitrile sulfide structures are sensitive to electron correlation effects, and the description of these latter effects is of crucial importance. Nonetheless, DFT can be a cost-effective approach for such molecules, and this approach was used to investigate decomposition processes. Nitrile sulfides are unstable in the condensed phase due to bimolecular reactions involving various sulfur transfer and cyclization processes between decomposition intermediates. Activation energy barriers of such reactions are small, below 10 kcal/mol, depending on the substituent, predicting a short lifetime for nitrile sulfides at ambient temperature. Dimerization to the unstable thiofuroxan is one of the major loss processes, and the instability and reactivity of thiofuroxan is responsible for the complicated decomposition mechanism. We note that in the case of nitrile oxides the dimerization to the stable furoxan derivatives are the dominant loss processes.<sup>12,13,22</sup> Nitrile sulfides have long been known from experiment to be stable to unimolecular decomposition,<sup>3</sup> and matrix IR and NRMS experiments have supported this. The present calculations are in agreement, suggesting that the generation of nitrile sulfides into the dilute gas phase for detailed spectroscopic and structural observation is still feasible, although remaining an experimental challenge.

**Acknowledgment.** We thank the Hungarian Scientific Research Fund (OTKA Grant F022031) and the Natural Sciences and Engineering Research Council of Canada (NSERC) for research and equipment grants in support of this work. T.P. thanks the Hungarian Soros Foundation for a travel grant and the Hungarian Academy of Sciences for the award of a János Bolyai Research Scholarship.

## References and Notes

- (1) Franz, J. E.; Black, L. L. *Tetrahedron Lett.* **1970**, 1381.
- (2) Paton, R. M. *Chem. Soc. Rev.* **1989**, 18, 33.
- (3) Wentrup, C.; Kambouris, P. *Chem. Rev.* **1991**, 91, 363.
- (4) Kambouris, P.; Plisnier, M.; Flammang, R.; Terlouw, J. K.; Wentrup, C. *Tetrahedron Lett.* **1991**, 32, 1487.
- (5) Maquestiau, A.; Flammang, R.; Plisnier, M.; Wentrup, C.; Kambouris, P.; Paton, R. M.; Terlouw, J. K. *Int. J. Mass Spectrom. Ion. Processes* **1990**, 100, 477.
- (6) Flammang, R.; Gerbaux, P.; Morkved, E. H.; Wong, M. W.; Wentrup, C. *J. Phys. Chem.* **1996**, 100, 17452.
- (7) Gerbaux, P.; Haverbeke, Y. V.; Flammang, R.; Wong, M. W.; Wentrup, C. *J. Phys. Chem. A* **1997**, 101, 6970.
- (8) Gerbaux, P.; Flammang, R.; Morkved, E. H.; Wong, M. W.; Wentrup, C. *Tetrahedron Lett.* **1998**, 39, 533.
- (9) Gerbaux, P.; Flammang, R.; Morkved, E. H.; Wong, M. W.; Wentrup, C. *J. Phys. Chem. A* **1998**, 102, 9021.
- (10) Bak, B.; Christiansen, J. J.; Nielsen, O. J.; Svanholt, H. *Acta Chem. Scand. A* **1977**, 31, 666.
- (11) Fehér, M.; Pasinszki, T.; Veszprémi, T. *Inorg. Chem.* **1995**, 34, 945.
- (12) Pasinszki, T.; Westwood, N. P. C. *J. Phys. Chem. A* **1998**, 102, 4939.
- (13) Pasinszki, T.; Westwood, N. P. C. *J. Phys. Chem. A* **2001**, 105, 1244.
- (14) Pasinszki, T.; Westwood, N. P. C. *J. Mol. Struct.* **1997**, 408–409, 161.
- (15) Pasinszki, T.; Westwood, N. P. C. *J. Phys. Chem.* **1996**, 100, 16856.
- (16) Geisel, M.; Mews, R. *Chem. Ber.* **1982**, 115, 2135.
- (17) Warren, J. D.; Lee, V. J.; Angier, R. B. *J. Heterocycl. Chem.* **1979**, 16, 1617.

- (18) Weinstock, L. M.; Davis, P.; Handelsman, B.; Tull, R. *J. Org. Chem.* **1967**, *32*, 2823.
- (19) Muhlbauer, E.; Weiss, W. (Farbenfabriken Bayer, A.-G.) Brit. Pat. 1,079,348, 1967; *Chem. Abstr.* **1968**, *68*, P69000w.
- (20) Pasinszki, T.; Westwood, N. P. C. *J. Electron Spectrosc. Relat. Phenom.* **2000**, *108*, 63.
- (21) Frisch, M. J.; Trucks, G. W.; Schlegel, H. B.; Scuseria, G. E.; Robb, M. A.; Cheeseman, J. R.; Zakrzewski, V. G.; Montgomery, J. A., Jr.; Stratmann, R. E.; Burant, J. C.; Dapprich, S.; Millam, J. M.; Daniels, A. D.; Kudin, K. N.; Strain, M. C.; Farkas, O.; Tomasi, J.; Barone, V.; Cossi, M.; Cammi, R.; Mennucci, B.; Pomelli, C.; Adamo, C.; Clifford, S.; Ochterski, J.; Petersson, G. A.; Ayala, P. Y.; Cui, Q.; Morokuma, K.; Malick, D. K.; Rabuck, A. D.; Raghavachari, K.; Foresman, J. B.; Cioslowski, J.; Ortiz, J. V.; Baboul, A. G.; Stefanov, B. B.; Liu, G.; Liashenko, A.; Piskorz, P.; Komaromi, I.; Gomperts, R.; Martin, R. L.; Fox, D. J.; Keith, T.; Al-Laham, M. A.; Peng, C. Y.; Nanayakkara, A.; Gonzalez, C.; Challacombe, M.; Gill, P. M. W.; Johnson, B.; Chen, W.; Wong, M. W.; Andres, J. L.; Gonzalez, C.; Head-Gordon, M.; Replogle, E. S.; Pople, J. A. *Gaussian 98*, Revision A.7; Gaussian, Inc.: Pittsburgh, PA, 1998.
- (22) Pasinszki, T.; Westwood, N. P. C. *J. Phys. Chem.* **1995**, *99*, 6401.
- (23) Pasinszki, T.; Westwood, N. P. C. *J. Am. Chem. Soc.* **1995**, *117*, 8425.
- (24) He, Z.; Cremer, D. *Int. J. Quantum Chem., Quantum Chem. Symp.* **1991**, *25*, 43. He, Z.; Cremer, D. *Theor. Chim. Acta* **1993**, *85*, 305.
- (25) Pople, J. A.; Head-Gordon, M.; Raghavachari, K. *Int. J. Quantum Chem., Quantum Chem. Symp.* **1988**, *22*, 377. Kraka, E.; Gauss, J.; Cremer, D. *J. Mol. Struct. (THEOCHEM)* **1991**, *80*, 95.
- (26) Pasinszki, T.; Westwood, N. P. C. Manuscript in preparation.
- (27) Calculated CN and NS bond lengths (B3LYP/cc-pVTZ): HC≡N, 1.146 Å; H<sub>2</sub>C=NH, 1.263 Å; HN=S, 1.572 Å; H<sub>2</sub>N-SH, 1.734 Å.
- (28) Gordy, W. *J. Chem. Phys.* **1947**, *15*, 305.
- (29) Howe, R. K.; Shelton, B. R. *J. Org. Chem.* **1981**, *46*, 771.
- (30) Harrit, N.; Holm, A.; Dunkin, I. R.; Poliakoff, M.; Turner, J. J. *J. Chem. Soc., Perkin Trans II* **1987**, 1227.
- (31) Holm, A.; Harrit, N.; Toubro, N. H. *J. Am. Chem. Soc.* **1975**, *97*, 6197.
- (32) Brupbacher, Th.; Bohn, R. K.; Jager, W.; Gerry, M. C. L.; Pasinszki, T.; Westwood, N. P. C. *J. Mol. Spectrosc.* **1997**, *181*, 316.